Bulletin of Earthquake Engineering
https://doi.org/10.1007/s10518-024-01900-5

ORIGINAL ARTICLE

Cost-effective topology optimization of masonry structure reinforcements by a linear static analysis-based GA framework

Antonio Pio Sberna[1] · Cristoforo Demartino[2] · Ivo Vanzi[3] · Giuseppe Carlo Marano[1] · Fabio Di Trapani[1]

Received: 27 October 2023 / Accepted: 11 March 2024

Abstract
The paper presents a novel optimization framework aimed at the minimization of seismic retrofitting-related costs for existing unreinforced masonry building structures. The framework provides topology optimization of reinforcements (reinforced plasters) to implement in masonry walls for the accomplishment of seismic safety checks under the reference seismic load combinations. Optimization is carried out by a genetic algorithm (GA) developed in MATLAB®, which controls a 3D finite element equivalent frame model of the masonry structure developed in OpenSees. The GA routine iterates the reinforcement configurations employing specific genetic operators. The feasibility of each candidate retrofitting solution is assessed by performing in-plane shear and flexural safety checks of masonry walls. The framework is finally tested with a case study masonry structure supposed to be made of average-quality or poor-quality masonry. Results will show that the proposed framework can effectively provide the minimization of seismic retrofitting costs for existing masonry structures, giving as output the optimal configuration of the reinforcements within the structural layout.

Keywords Seismic retrofitting · Genetic algorithm · Structural optimization · Reinforced plasters · Masonry · Existing buildings

✉ Fabio Di Trapani
fabio.ditrapani@polito.it

[1] Department of Structural, Building and Geotechnical Engineering, Politecnico Di Torino, Corso Duca Degli Abruzzi 24, 10129 Turin, Italy

[2] Department of Architecture, Roma Tre University, Via Aldo Manuzio, 68L Rome, Italy

[3] Department of Engineering and Geology, University of Chieti-Pescara "G. D'Annunzio", Pescara, Italy

Published online: 13 May 2024

1 Introduction

In Italy, and the Mediterranean area, a large number of buildings are located in earthquake-prone zones. Unreinforced masonry structures are widespread in these territories. In many cases, these are really old buildings, not conceived to sustain earthquake loads. Seismic events that occurred in the last decades (e.g. L'Aquila in 2009 and Amatrice in 2016, in Italy) demonstrated that seismic risk associated with these structures can be relevant, mainly because of their significant vulnerability. The huge post-earthquake reconstruction costs led Italian, and other governments of countries in seismic-prone areas to allocate funds to prevent earthquake-related disasters by reducing the seismic vulnerability of the existing built heritage. For what concerns unreinforced masonry structures, many effective reinforcements and retrofitting techniques are available as potential technical solutions (e.g. reinforced plasters, grout injections, prestressed ribbons, composite materials, etc.) to supply additional flexural and shear resistance to the walls. On the other hand, formal design criteria addressing the retrofit intervention towards the obtainment of a required performance (e.g. a target safety level or a target structural behaviour) are substantially unavailable. The retrofit design process is mainly based on a trial-and-error approach, which starts from the engineer's intuition and experience. Such a non-engineered approach has a double drawback. The first is the difficulty of individuating a suitable retrofitting configuration unless making several iterations. In fact, the reinforcement of a wall can involve an increase of the mass or the stiffness or both mass and stiffness, modifying the demand on the structural element (which can even attract more force). Non-negligible recursive design issues can arise in these cases. The second, and related to the previous point, is that there is no control over retrofitting costs. Namely, there is no way to know if a candidate retrofitting configuration is also the one associated with the minimum possible cost. Overestimation of reinforcement is then rather common in these cases, generating additional costs associated with major invasiveness and downtime. Engineered design methodologies addressing a specific target strongly emerge as a need in this field. Over the years, the capability offered by computational intelligence has been more and more employed to solve large and complex structural engineering problems (Quaranta et al. 2020; Falcone et al. 2020). Many applications addressed sizing, shaping, and topology optimization for the design of new structures (Lagaros et al. 2002; Govindaraj and Ramasamy 2005, 2007; Mitropoulou et al. 2011; Papavasileiou and Charmpis 2016; Babaei and Mollayi 2016; Pham and Hong 2022; Kanyilmaz et al. 2022), founding those evolutionary algorithms, such as genetic algorithms, are suitable to minimize noisy or discrete objective functions.

More recently, evolutionary algorithms started being applied to retrofit design optimization of existing structures. The major interest regarded reinforced concrete structures, for instance, the minimization of the use of carbon fiber reinforced polymers (CFRP) as reinforcements (e.g. Chaves and Cunha 2014; Seo et al. 2018; Mahdavi et al. 2019; Falcone et al. 2019). More recently, Papavasileiou et al. (2020) implemented a novel framework based on a genetic algorithm (GA) for optimizing the implementation costs of three different retrofitting techniques (steel-jacketing, concrete jacketing, and steel braces) for encased steel–concrete composite columns. Similarly, Di Trapani et al. (2020), proposed a novel framework aimed at minimizing steel jacketing retrofitting costs for RC columns. Afterward, Di Trapani et al. (2021) extended their optimization framework capability to both ductility-critical and shear-critical RC frame structures. More recently, Minafò and Camarda (2022) proposed a GA-based optimization procedure for the minimization of the costs of implementation of buckling-restrained braces (BRB) in reinforced concrete

frames. Lastly, Di Trapani et al. (2022) implemented a new genetic algorithm-based framework pinpointing the optimal retrofitting configuration of FRP wrapping of columns and steel bracing in RC structures taking into account both the costs and the expected annual economic losses during the service life. The literature review mentioned so far highlights a growing interest in the application of soft-computing techniques to solve retrofitting design issues. Also, the obtained results demonstrate that this way of approaching the design of seismic retrofit is effective in reducing the costs and invasiveness of the interventions. However, the considered scientific literature reveals an evident lack of experience in the potential application of these soft-computing techniques to the optimization of unreinforced masonry structure seismic retrofit, although the design of reinforcement for masonry structures is not straightforward, as demonstrated by recent studies addressing refined fine element-based topology optimization of fiber reinforcement of masonry walls (Bruggi et al. 2013, 2014; Bruggi and Gabriela 2015). Based on these considerations, the current paper proposes a new computational intelligence-based framework supporting the design of seismic reinforcement of existing masonry structures characterized by adequate structural regularity, by minimizing their cost under the constraint of satisfying the safety checks provided by the current technical codes. The optimization algorithm is consistent with the prescriptions and the capacity models provided by the Italian National Technical Code (NTC 2018) for the reinforcement of masonry walls, but the framework is robust enough to consider different, or more general, capacity models and safety verification rules. In the paper, the focus is made on the very common reinforced plaster technique. The objective function provided within the optimization algorithm evaluates the intervention costs considering the surface of the walls where reinforced plasters are implemented. The final output of the framework is the optimal retrofitting configuration, namely the topology of walls needing reinforcements associated with the minimum cost and satisfying the safety checks provided by the technical code.

The optimization procedure is carried out by linking the GA optimization routine developed in MATLAB® with an equivalent frame 3D finite element (FE) model analyzed through the OpenSees software platform (McKenna et al. 2000). The performance of each tentative solution (namely a candidate configuration for the seismic retrofit), is controlled in terms of in-plane flexural and shear safety checks under the reference seismic design forces. The proposed framework is tested on a 2-storey masonry building supposed to be made of two different typologies of masonry (squared stone unit masonry and coursed tender stone masonry). Results demonstrate that in both cases the application of the proposed GA-based optimization framework can effectively reduce the extent of seismic upgrading interventions enabling cost-saving associated with downtime and invasiveness reduction.

2 Masonry reinforcement with reinforced plasters

2.1 General features of reinforced plasters

The in-plane reinforcement of masonry walls can be performed according to different techniques (Priestley and Seible 1995). Among these, the use of composite materials [e.g., fiber-reinforced polymers (FRP) or fiber-reinforced cementitious matrices (FRCM)] found significant applications for masonries with regular textures. Similarly, the application of prestressed steel ribbons (CAM) has been used especially for masonry buildings belonging to the historical heritage, or in the case of heterogenous masonries. At the same time,

the use of reinforced plasters is very common due to their relatively low cost and ease of implementation in comparison with the other techniques. This retrofitting methodology entails the application of a reinforcement net typically made of steel (Fig. 1a) or Glass Fiber-Reinforced Polymer (GFRP) (e.g. Fig. 1b) on both faces of the masonry wall, embedded in a thick layer (40–100 mm) of special cement mortar (Fig. 1c). In the case of GFRP, the net is made up of fiber-glass wires bonded together with an epoxy resin (Gattesco et al. 2015; Gattesco and Boem 2015). The net shape is created by intertwining the transversal wires with the longitudinal ones. During the implementation, after the demolition of the existing plasters and the outermost layer of mortar joints, the net is placed on the surface of the wall and a layer of shotcrete is implemented. The tiers of reinforced plasters are coupled with underlying the masonry wall by dowels (Fig. 1c) to prevent debonding and provide some additional confining action.

2.2 Capacity models and in-plane safety checks

Differently from FRCM, detailed analytical capacity models for masonry walls reinforced by reinforced plasters are substantially not available in the literature, while Eurocode 8—Part 3 (2004b) provides only general recommendations. The Italian Technical Code (NTC 2018) allows the modeling of the effect of reinforced plasters in a simplified way. This provides increasing the original mechanical properties of the masonry (strength and elastic moduli) by an amplification factor (> 1), which in the following will be called α_r. The α_r coefficient simultaneously applies to the masonry compressive strength (f_m), shear strength (τ_{0m}), Young modulus (E_m), and shear modulus (G_m), so that:

$$\begin{aligned} \overline{f}_m &= \alpha_r \cdot f_m \\ \overline{\tau}_{0m} &= \alpha_r \cdot \tau_{0m} \\ \overline{E}_m &= \alpha_r \cdot E_m \\ \overline{G}_m &= \alpha_r \cdot G_m \end{aligned} \tag{1}$$

where the over-signed terms represent the mechanical properties of reinforced walls. The α_r coefficients are defined as a function of the original typology of masonry where this intervention is realized. For the reinforced plaster intervention α_r coefficients range between 1.2 and 2.5, as shown in Table 1. The same approach can be applied in the case of wall reinforcements by grout injection or reinforced stitching of mortar joints (Table 1),

Fig. 1 Application of reinforced plasters to masonry walls: **a** electro-welded steel net; **b** GFRP; **c** scheme of arrangement of the reinforcement

Table 1 Amplification factors (α_r) for different masonry typologies and reinforcement interventions

Masonry typology	Reinforced plasters	Grout injection	Strengthening of mortar joints
Non-uniform masonry	2.5	2.0	1.6
Rough-hewn ashlar masonry with non-homogeneous	2.0	1.7	1.5
Split stone masonry with regular texture	1.5	1.5	1.4
Irregular tender stone masonry	1.7	1.4	1.1
Coursed tender stone masonry	1.5	1.2	1.2
Squared stone block masonry	1.2	1.2	–
Solid brick masonry	1.5	1.2	1.2
Hollow unit masonry	1.3	–	–

however, in the case of reinforced plasters, the original thickness of the wall (t) is increased by the thickness of the reinforced plaster, so that the final thickness $\bar{t}$ will be:

$$\bar{t} = t + 2 \cdot t_{rp} \tag{2}$$

where t_{rp} is the thickness of the reinforced plaster on each side of the wall.

In-plane safety checks of reinforced masonry (flexure and shear) are simply carried out by using the upgraded thickness of the wall ($\bar{t}$) and design resistances ($\bar{f}_d$ and $\bar{\tau}_{0d}$), which are defined as:

$$\begin{aligned} \bar{f}_d &= \alpha_r \cdot f_d = \frac{\alpha_r \cdot f_m}{CF \cdot \gamma_M} = \frac{\bar{f}_m}{CF \cdot \gamma_M} \\ \bar{\tau}_{0d} &= \alpha_r \cdot \tau_{0d} = \frac{\alpha_r \cdot \tau_{0m}}{CF \cdot \gamma_M} = \frac{\bar{\tau}_{0m}}{CF \cdot \gamma_M} \end{aligned} \tag{3}$$

where CF and γ_M are respectively the confidence factor and the partial safety factor defined according to the technical code. With reference to Fig. 2, the ultimate flexural resistance (M_u) is computed as:

$$M_u = \frac{\sigma_0 \cdot \ell^2 \cdot \bar{t}}{2} \cdot \left(1 - \frac{\sigma_0}{0.85 \cdot \bar{f}_d}\right) \tag{4}$$

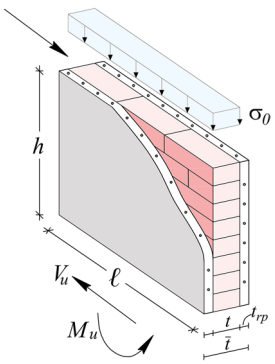

Fig. 2 Reference scheme for the evaluation of in-plane ultimate moment and shear of a reinforced masonry wall

where ℓ is the length of the wall, and $\sigma_0 = N_0/(\ell \cdot t)$ is the average compressive stress (N_0 being the current axial force acting on the wall). For an unreinforced wall, the original design strength (f_d) and thickness (t) are used in Eq. (4).

The ultimate shear resistance is evaluated according to the model by Turnšek and Čačovič (1971) as follows:

$$V_u = \frac{\ell \cdot \bar{t} \cdot 1.5 \cdot \bar{\tau}_{0d}}{b} \cdot \sqrt{1 + \frac{\sigma_0}{1.5 \cdot \bar{\tau}_{0d}}} \tag{5}$$

where $b = h/\ell$ is the aspect ratio of the wall ($1 \le b \le 1.5$). Again, if the wall is not reinforced, the original shear design strength (τ_{0d}) and thickness (t) are used in Eq. (5). Equations (4–5) are generally conservative, but they can be eventually updated to consider the effect of T-junctions in correspondence of orthogonal walls.

A comparison of the unreinforced and reinforced flexural and shear interaction domains ($N_0 - M_u$) and ($N_0 - V_u$) by Eqs. (4) and (5) is represented in Fig. 3 for a sample masonry wall. It is noteworthy observing that capacity models in Eqs. (4) and (5), can be replaced anytime by different, or more refined models without any drawback for the below-discussed optimization framework.

3 Optimization framework

3.1 Working principles

The optimization procedure herein proposed is based on the genetic algorithm metaheuristic technique. This class of soft-computing algorithms analyzes the research space through the handling of a set of variables that are gathered in a so-called design vector. Each tentative solution represents a possible retrofitting configuration. The procedure followed in the framework is schematically represented in Fig. 4. The decision variables, namely the parameters to optimize, are defined at the beginning, once one (or more) strengthening techniques are chosen. This will include the position of the reinforcement and its sizing (if

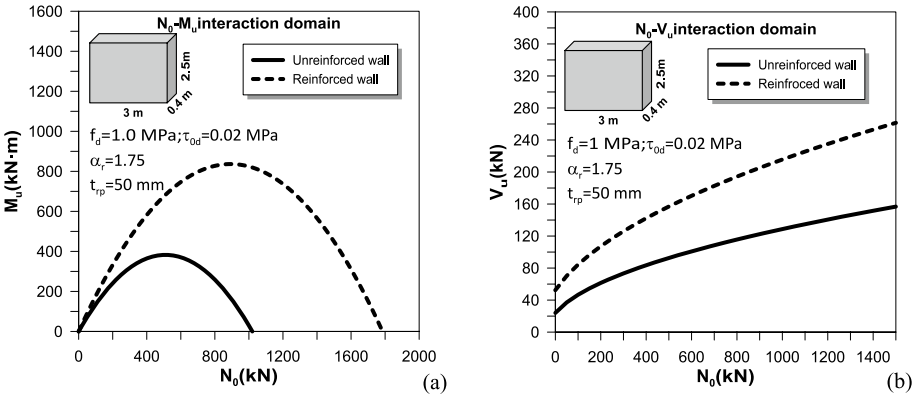

Fig. 3 Unreinforced and reinforced flexure and shear interaction diagrams for a sample masonry wall: **a** $N_0 - M_u$; **b** $N_0 - V_u$

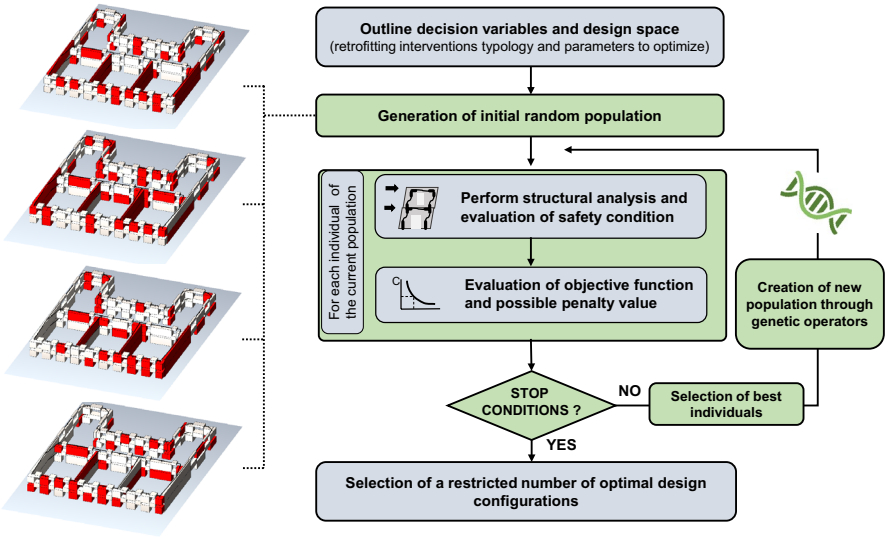

Fig. 4 Flowchart of the optimization framework

needed). The algorithm starts generating a random initial population of design vectors (tentative solutions) and evaluates the objective function for each individual. For the current application, the objective function will compute the material and manpower cost to implement the reinforcement at the global level, namely the reinforcement of masonry piers. The fittest individuals are then selected, and through the application of the genetic operators, a new generation of tentative solutions is created. Reinforcements for local failure mechanisms are not included in the design optimization process as their design is independent and typically does not need optimization.

As can be observed from Fig. 4, the optimization algorithm is the core of the framework, but two fundamental engineering decision phases are left to the designer. The first one is the initial selection of the design variables, which allows the possible definition of a restricted design space (e.g. limiting the optimization to a portion of the building or reducing the number of parameters to be optimized). This operation significantly influences the potential reduction of the computational cost. In the last phase, a restricted number of optimized solutions with similar fitness are compared. The most suitable is then selected by the designer considering the technical feasibility. The main features of the proposed framework are described in detail in the following sections.

3.2 Design vector encoding

The optimization algorithm aims to pinpoint the topology of the walls to be reinforced so that the retrofitting cost is minimized. The topology optimization is performed by using binary variables to encode the presence or not of the reinforcement on each wall. All the decision variables are gathered in the design vector **b** so defined:

$$\mathbf{b} = \left[\ldots \; b_{ij} \; \ldots \right]^T \tag{6}$$

where b_{ij} is a Boolean variable assuming the value 1 if the wall is retrofitted and 0 if not, namely:

$$b_{ij} \in B = (0\ 1) \tag{7}$$

where B is the binary set. The subscripts i and j denote the position of the wall in plan and the story, respectively. It is noteworthy observing that walls included in the design vector can have different material properties, and so structures arranged with different typologies of masonry can be also handled by the optimization framework. In order to reduce the dimension of the research space, and so the computational burden required for the analysis, each Boolean variable can also represent a cluster of adjoining walls. Clustering is quite helpful to implement some architectural restraints, to which the seismic intervention must comply.

The choice of the optimization algorithm procedure is felt on genetic algorithms since the approach is particularly efficient in handling a research space defined by Booleans. The implementation or not of the reinforcement intervention as encoded in the design vector is fulfilled by modifying the geometrical and mechanical properties of the walls as provided by Eqs. (1–3).

3.3 Definition of the objective function

The objective function (OF) to be minimized, also called fitness function, evaluates the costs associated with the implementation of the reinforced plaster strengthening intervention. Since the cost is strictly related to the surface of retrofitted walls, the objective function simply appraises the total surface of reinforced plasters that is encoded by the design vector of each individual. To consider the feasibility of each solution (namely if all the safety checks are passed for an individual), the fitness function involves a penalty function, that is used to fictitiously increase the fitness value of unfeasible individuals. The objective function ($OF(\mathbf{b})$) is, therefore defined as:

$$OF(\mathbf{b}) = C(\mathbf{b}) + \Pi \tag{8}$$

where C is the cost function and Π the penalty function. As can be noted, the objective function and the cost function depend on the design vector ($\mathbf{b}$) representing each individual.

Assuming that the cost per unit surface of reinforced plasters is a constant, the cost function here used will consider only the surface of reinforced plasters, so that:

$$C = \sum_{i=1}^{n_{rw}} A_{rp,i} \tag{9}$$

where $A_{rp,i}$ is the surface of reinforcement applied to the i-th reinforced wall, and n_{rw} is the number of reinforced walls. It is noteworthy observing that, since reinforced plasters are applied at both sides, the surface $A_{rp,i}$ corresponds to twice the area of the reinforced wall panel ($A_{rw,i}$), so that:

$$A_{rp,i} = 2 \cdot A_{rw,i} \tag{10}$$

The penalty function is instead defined as:

$$\Pi = p \cdot \sum_{i=1}^{n_a} \left(\sum_{j=1}^{n_{wf}} A_{wf,j} + \sum_{k=1}^{n_{ws}} A_{ws,k} \right)_i \tag{11}$$

where $A_{wf,j}$ and $A_{ws,k}$ are the areas of the n_{wf} and n_{ws} walls having a strength capacity/demand ratio lower than 1, with respect to flexure and shear safety checks respectively. The i index of the external sum counts the n_a seismic analyses performed, namely each different direction and sign considered for the seismic forces. Finally, p is a penalty coefficient fictitiously magnifying the weight of the sums Eq. (11). The magnification of the penalty function allows the algorithm to be aware of the unfeasible individual's genomes when generating the new population. Obviously, for a feasible individual one obtains $\Pi = 0$.

3.4 Genetic operator subroutines

Genetic algorithms are a population-based class of metaheuristic algorithms inspired by the natural selections of species (Goldberg 1989; Holland 1992). The main engine of optimal seeking is based upon the concept of survival of the fittest individuals. The algorithm starts generating a random population of tentative solutions (namely candidate retrofitting configuration) and evaluates the fitness associated with them. The pursuit of the research space minima is achieved by selecting the best tentative solutions and creating new individuals starting from their design vectors (namely the genome) through the parent selection, crossover, and mutation genetic operators. The first of these operators selects the parent tentative solutions, the second mixes the genomes of tentative solutions, and the third introduces some randomness in the genome of child individuals to prevent the algorithm stuck into local minima and enhance the genetic diversity of the population. A scheme describing the application of the genetic operators in creating a new individual is illustrated in Fig. 5. The parent selection operator makes use of tournament selection (Goldberg and Deb 1991). Within the current population, k individuals are randomly chosen, and their fitness is evaluated. Among these individuals, the best two (in terms of fitness) are employed as parents. The parameter k is commonly called tournament size. The balancing of this parameter allows controlling of the selective pressure, namely a reduction of k will allow individuals with slightly poorer fitness to generate offspring. On the other hand, an increase of k will permit only the fittest individuals to pass the generation, with a consequent reduction in the diversity of the genetic pool.

A *single-point crossover* (Kora and Yadlapalli 2017) is used to mix the parents' genome. It selects a random *crossover point* along the design vector and generates the offspring by taking the first part of the genome from the beginning to the crossover point from the first

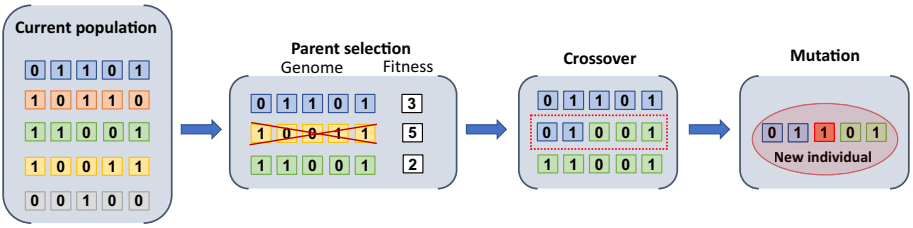

Fig. 5 Schematic representation of the application of the genetic operators in creating a new individual

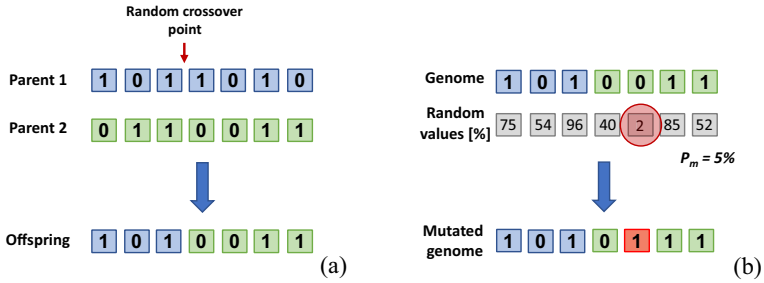

Fig. 6 Working principle of the genetic operators: **a** single-point crossover; **b** mutation

parent, and the remaining part from the crossover point to the end of the genome from the second parent (Fig. 6a). In this way, the new individual has inherited a portion of the genome from both parents but keeps intact the characteristics of locality. This means that if a portion of the genome is good in terms of its effect on overall fitness, this can be passed on to the offspring intact.

Finally, the mutation operator introduces slight changes in the structure of the offspring genome. This prevents the algorithm from being stuck in local minima and promotes the diversity of populations (Squillero and Tonda 2016). The mutation is also useful to recover good genetic material that may be lost during selection and crossover operations.

This subroutine operates by setting first a mutation percentage probability (p_m). Then a random integer percentage number between 0 and 100% is drawn for each decision variable (Fig. 6b). If the percentage number associated with a decision variable is smaller than the mutation probability, the value of the variable, which is a Boolean variable, is switched. The value of the mutation probability should be chosen properly since low values can reduce the effectiveness of the operator with which the exploitation phase is mainly entrusted. On the other hand, high mutation probability can lead to a radical modification of the genome, making useless the previous selection and crossover operation. Typical values of mutation probability, for this kind of problem, are commonly fixed around 1–5%.

The framework automatically interfaces MATLAB® with OpenSees. For each candidate solution, a set of MATLAB subroutines modify the OpenSees model according to the genome collected in the design vector. The model of each individual is then moved to OpenSees for structural analysis. Results are post-processed in MATLAB for safety checks, fitness evaluation, and application of the genetic operators. In the last stage, the survival selection operator is applied. The latter selects the new population to be analyzed based on a fitness ranking of the individuals, in which only the better ones are used as the new population. The optimization routine is stopped when no further cost reductions are obtained over a certain number of generations. A comprehensive flowchart of the GA framework is illustrated in Fig. 7.

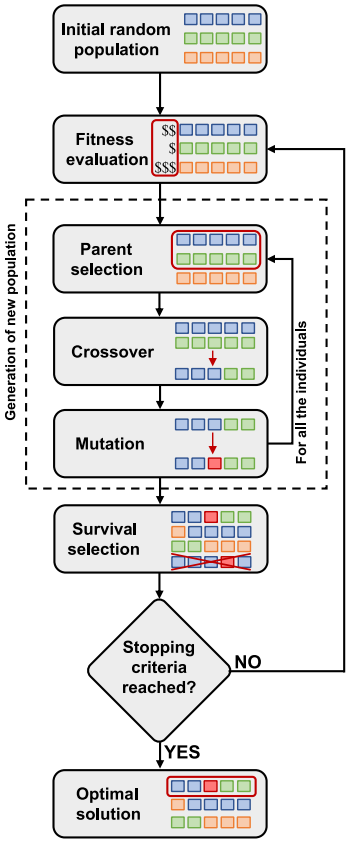

Fig. 7 Flowchart of the genetic algorithm framework

4 Structural modelling and seismic analysis

4.1 Reference model for the masonry building structure

The optimization algorithm is interfaced with an FE solver to perform the structural analysis and the assessment of each tentative solution. For the current study, the optimization algorithm is interconnected with the OpenSees software platform. The masonry structure is defined as an elastic 3D-frame model by employing the Equivalent Frame Method (EFM), which has proven to be reliable for regular masonry building structures (Cattari et al. 2022; Camata et al. 2022). According to the EFM, the structure is subdivided into masonry panels and spandrels, which are connected through rigid links. The actual deformable length of the walls is evaluated as a function of the opening shape, according to the method by Braga and Dolce (1982). The remaining unreformable parts are considered as rigid links. In the current study, the elastic portion of masonry walls and spandrels are modelled as Timoshenko beams, using the *ElasticTimoshenkoBeam* elements implemented in OpenSees. The connection between the orthogonal walls is modelled through rigid trusses using the *rigidLink bar* element. A rigid diaphragm constraint is applied to the floors. In the FE model, reinforced plasters are modeled according to Eqs. (1–2), that is by modifying the elastic Young's and shear moduli, and the

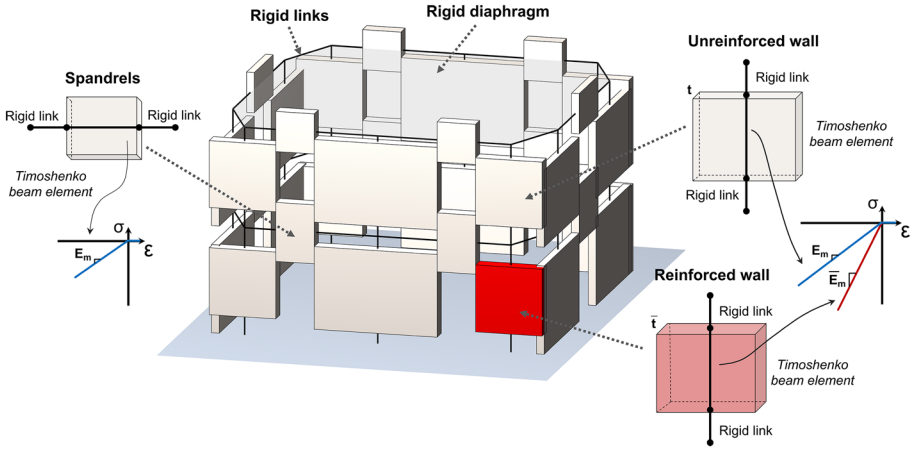

Fig. 8 Reference OpenSees FE model of the masonry structure

thickness of the element. The modification of the wall thickness is not only reflected as an increase of the stiffness of the element but also the structural weight and the corresponding masses are updated. A scheme of the reference modeling approach is provided in Fig. 8. It is noteworthy to observe that the choice of a linear EFM model, although introducing several simplifications and generally being conservative, allows a noticeable reduction of the computational effort, which is a fundamental aspect to the feasibility of the framework.

4.2 Seismic analysis

The current optimization framework is conceived to be combined with linear seismic analysis (linear equivalent static analysis or response spectrum analysis), to determine the seismic demand in terms of internal forces on the frame elements. The choice of adopting linear seismic analyses differs from some recent studies of the authors (e.g. Di Trapani et al. 2020, 2021, 2022) where nonlinear static analysis is used. However, in the framework of the algorithm's efficiency, the adoption of a linear analysis allows a huge reduction of the computational time needed to get the optimal solution. This kind of approach must be interpreted as a fast optimization of the reinforcement. The inelastic performance of the optimal retrofitting solution can anytime be assessed by a nonlinear analysis.

For structures with a regular distribution of masses and stiffness over the height Eurocode 8 (2004a), and Italian Technical Code (NTC 2018), allow performing the very simple equivalent static seismic analysis. The latter is briefly recalled as it was used to analyze the case studies presented in the following sections. According to the equivalent static seismic analysis, the total horizontal seismic load is evaluated as:

$$F_h = S_d(T_1) \cdot (W/g) \cdot \lambda \tag{12}$$

where $S_d(T_1)$ is the design spectral acceleration in correspondence with the vibration period T_1, W is the total weight of the structure according to the seismic combination of loads, g is the gravitational acceleration, and λ is a corrective factor that is 0.85 if $T_1 \leq 2\ T_c$ (T_c

being the corner period) and the structure has more than two stories, or 1 otherwise. The fundamental period of vibration of structure (T_1) can be estimated in a simplified way as $T_1 = c_1 \cdot H^{3/4}$, where H is the total height of the building in meters and c_1 is 0.05 for masonry structures. The total seismic load (F_h) is linearly distributed over the height of the building proportionally to the product of the stories' height and weight. For each candidate solution, the combination of the seismic forces simultaneously acting in the two horizontal orthogonal directions (X and Z) is considered. Specifically, eight analyses are performed by applying 100% of the seismic load in the main direction (X or Z) and 30% in the perpendicular one. Positive and negative verses of actions are considered so that the following combinations are obtained for each analyzed individual:

$$\begin{cases} +1.0 \cdot E_X \pm 0.3 \cdot E_Z \\ -1.0 \cdot E_X \pm 0.3 \cdot E_Z \\ +0.3 \cdot E_X \pm 1.0 \cdot E_Z \\ -0.3 \cdot E_X \pm 1.0 \cdot E_Z \end{cases} \tag{13}$$

Seismic forces are applied at the center of mass of each floor. The accidental eccentricity of the center of mass is here neglected for the sake of simplicity.

4.3 Safety checks

Safety checks of masonry walls are carried out for the maximum in-plane flexural capacity (M_u) and shear capacity (V_u) of masonry walls. Flexural and shear demands (M_d) and (V_d) on the walls are obtained from the seismic analysis of each candidate solution. For each analysis and wall, safety checks will simultaneously verify that:

$$\frac{M_u}{M_d} \geq 1 \qquad \& \qquad \frac{V_u}{V_d} \geq 1 \tag{14}$$

where M_u and V_u are evaluated according to Eqs. (4–5). Local out-of-plane mechanisms are not accounted by Eq. (14), however, they can be added as an additional condition without losing the validity of the framework.

An effective representation of the current flexural and shear safety checks can be performed by defining the dimensionless domains. For the flexural domain, this can be done by normalizing Eqs. (4) by $f_d \cdot \ell^2 \cdot t$, that is:

$$m_u = \frac{M_u}{f_d \cdot \ell^2 \cdot t} = 0.5 \cdot \frac{\sigma_0}{f_d} \cdot \left(1 - \frac{\sigma_0}{0.85 \cdot f_d}\right) \tag{15}$$

By defining the normalized axial load as $n_0 = \sigma_0 / f_d$, from Eq. (15) one obtains:

$$m_u = 0.5 \cdot n_0 \cdot \left(1 - \frac{n_0}{0.85}\right) \tag{16}$$

Similarly, the dimensionless shear domain can be defined by normalizing Eqs. (5) by $b/1.5 \cdot \tau_{0d} \cdot \ell \cdot t$, so that:

$$v_u = \frac{V_u \cdot b}{1.5 \cdot \tau_{0d} \cdot \ell \cdot t} = \sqrt{1 + \frac{\sigma_0}{1.5 \cdot \tau_{0d}}} = \sqrt{1 + n_v} \tag{17}$$

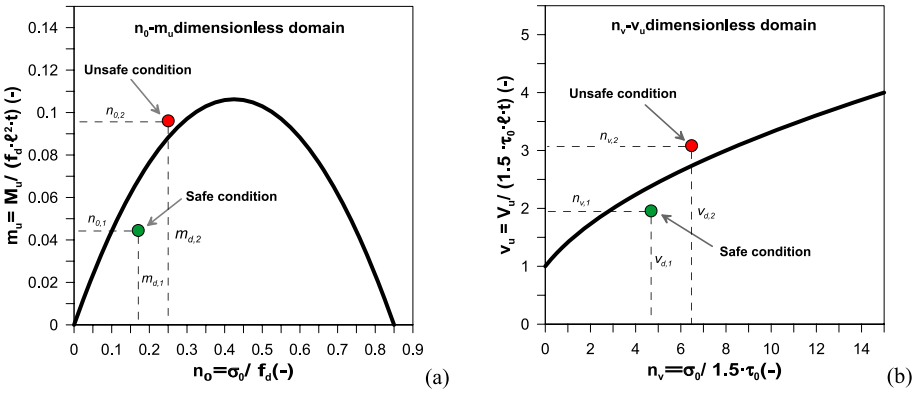

Fig. 9 Dimensionless interaction domains and safety checks: **a** flexure ($n_0 - m_u$); **b** shear ($n_0 - v_u$)

where n_v is the ratio between the average normal stress and the diagonal tensile strength ($1.5 \cdot \tau_{0d}$) of the wall, that is:

$$n_v = \frac{\sigma_0}{1.5 \cdot \tau_{0d}} \tag{18}$$

In Eqs. (15) and (17), the geometrical and mechanical properties of the masonry f_d, τ_{0d}, and t are respectively changed in $\overline{f}_d$, $\overline{\tau}_{0d}$, and $\overline{t}$ if the wall is reinforced.

Dimensionless domains are defined by Eqs. (16) and (17) by varying n_0 and n_v. They allow to define unique interaction domains to graphically represent flexural and shear capacities of all the masonry walls of a structure, regardless of their geometrical dimensions and resistances (Fig. 9). The demand points are expressed by the pairs n_0, m_d for flexure and n_v, v_d for shear, where m_d and v_d are defined as:

$$m_d = \frac{M_d}{f_d \cdot \ell^2 \cdot t} \qquad v_d = \frac{V_d}{\ell \cdot t \cdot 1.5 \cdot \tau_{0d}} b \tag{19}$$

Each demand point on the dimensionless diagram represents the condition of a wall with respect to the safety limits for a specific load combination. If one (or more) safety checks are not passed the entire candidate solution is defined as unfeasible and is treated according to the penalty approach defined in Eq. (11). The use of dimensionless diagrams is particularly suitable to gather in a sole diagram of the safety checks for each wall and load combination.

5 Case study tests

5.1 Details of the case study structure

The proposed optimization framework is tested with the case study of a 3D masonry structure consisting of a C-shape two-storey building having planar dimensions of 27.80 × 12.5 m and with a total height of 8 m (Fig. 10). The structure has a symmetry axis

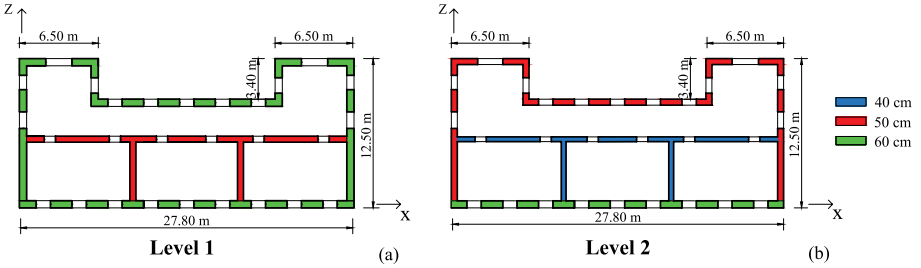

Fig. 10 Geometrical dimensions of the case study structure: **a** Ground floor; **b** First floor

along the Z direction. The optimization framework is tested on the building by making two different assumptions for the masonry constituting the wall. In the first case, the structure is supposed to be made of squared stone block masonry (SSM), and in the second case of coursed tender stone masonry (TSM). The average values of the mechanical properties of the two types of masonries are reported in Table 2. The design values of the compressive strength (f_d) and shear strength (τ_{0d}) are obtained by Eq. (3) assuming a knowledge level 2, so that CF = 1.2. The partial safety factor is $\gamma_m = 2$.

For both SSM and TSM the application of reinforced plasters implies an increment coefficient $\sigma_R = 1.5$ according to the Italian NTC (2018) (Table 1). The mechanical properties of the reinforced masonries are reported in Table 3.

The building is supposed to be located in Cosenza (Italy) with a soil type C. The reference nominal life (V_N) is 100 years. The resulting return period is $T_R = 975$ years. The fundamental vibration period evaluated for the structure is $T_1 = 0.23$ s. Given the regularity of the building over the height, the behaviour factor (q) is set equal to 3 according to NTC (2018). The reference elastic and design spectra are depicted in Fig. 11.

It is assumed that reinforced plasters are implemented with a thickness of $t_{rp} = 50$ mm for each side of retrofitted walls. Floors are supposed to be rigid in their plan so that a rigid diaphragm constraint is imposed at the floor nodes. A unit load of $q_{floor1} = 5.6$ kN/m^2 and $q_{roof} = 5.0$ kN/m^2 is evaluated for the slab of the first floor and the roof respectively (seismic combination). The resulting total weight of the structure used for the seismic analysis is 9504 *kN*. In the equivalent frame model, vertical loads are modelled as point loads applied to the top node of each vertical element. Loads from the slabs are transferred to the nodes as a function of the respective tributary areas.

Table 2 As-built mechanical properties of masonry for the case-study structures

Masonry typology	f_m (MPa)	τ_{0m} (MPa)	E_m (MPa)	G_m (MPa)	w (kN/m^3)
Squared stone blocks (SSM)	3.2	0.065	1750	575	21
Coursed tender stone (TSM)	2.6	0.060	1410	450	15

Table 3 Mechanical properties of masonry strengthened by reinforced plaster for the case-study structures

Masonry typology	$\overline{f}_m$(MPa)	$\overline{\tau}_{0m}$(MPa)	$\overline{E}_m$(MPa)	$\overline{G}_m$(MPa)	w (kN/m^3)
Squared stone blocks (SSM)	5.4	0.11	2975	977	21
Coursed tender stone (TSM)	3.9	0.09	2115	675	15

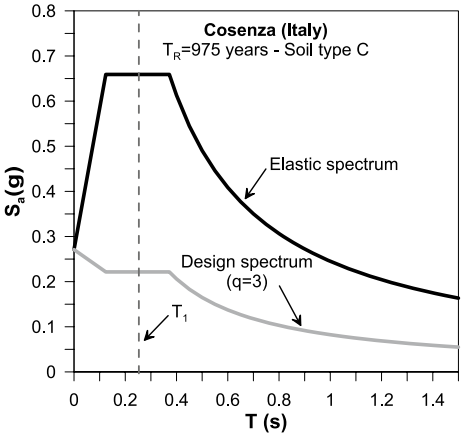

Fig. 11 Reference elastic and design spectra

5.2 Preliminary assessment of as-built structures and non-optimized retrofitted structures

Seismic analyses and safety checks of the as-built structures have been carried out according to what was described in the previous section. This preliminary assessment allowed evaluating the walls that were not satisfying flexural and shear safety checks under the reference seismic demand. An overall graphical representation of the safety checks of the structure in the as-built configuration is depicted in Fig. 12, where different colors are used to denote flexure, shear, and flexure/shear failures of SSM and TSM structures.

For the SSM structure, 18 out of 78 walls (23%) did not satisfy shear and flexural verifications. For the TSM structure, the walls not passing safety checks were 28, which is 36% of the total. Details about the outcomes of the safety checks of the as-built structures are reported in Table 4. Assessment of SSM and TSM structure was repeated by applying reinforced plasters to all the walls missing the safety checks. Considering both sides of the walls the surfaces subject to the application of reinforced plasters were 349.7 m^2 and 602 m^2 for the SSM and TSM structure respectively. In both cases this allowed the walls to pass safety checks, although the design of the reinforcement was carried out without any optimization criterion. Assuming an average retrofitting cost of 200 €/m^2, the total estimated cost for the retrofitting interventions was 69,940 € and 120,480 € for the SSM and TSM structure respectively (Table 5). Results of safety checks for every wall and load combination are graphically displayed in Figs. 13, 14, where the outcomes of the unreinforced and reinforced structures are overlapped within the dimensionless domains.

5.3 Results of the application of the optimization framework

The proposed optimization framework has been tested with the case study structures above described. Some preliminary assumptions have been made to reduce the dimension of research space and to avoid unpractical retrofitting configurations. In particular, the adjoining walls were grouped into clusters (Fig. 15), so that a cluster of walls became the unit element of the design vector. Besides the reduction of the computational effort, this assumption avoids considering solutions providing scattered reinforcement of the facades. Therefore, the 78 masonry walls were converted into 42 clusters. This allowed reducing

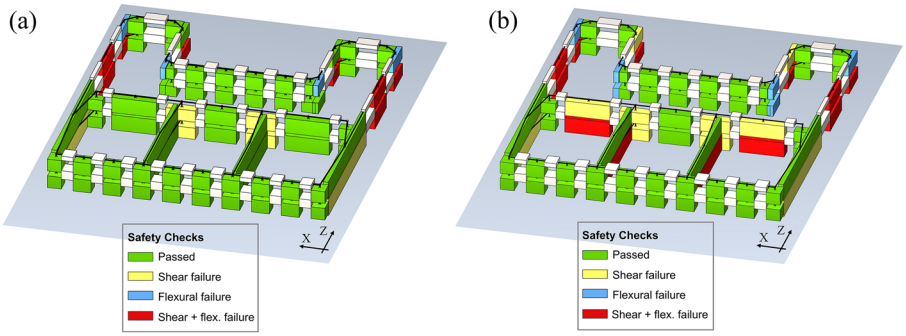

Fig. 12 Assessment of the structure in the as-built configuration: **a** Squared stone masonry (SSM); **b** Tender stone masonry (TSM)

Table 4 Outcomes of safety checks for the as-built squared stone masonry (SSM) and tender stone masonry (TSM) structures

Structural model	Walls failing in flexure (#)	Walls failing in shear (#)	Walls failing in flexure and shear (#)	Total number of walls (#)
SSM (As-built)	4	6	8	72
TSM (As-built)	6	10	12	72

Table 5 Reinforcement details and cost of non-optimized retrofitting interventions

Structural model	Reinforced Walls (#)	Walls failing in flexure and/or shear (#)	Total surface of reinforced plasters (m^2)	Estimated retrofitting cost (€)
SSM (Non-opt. reinforced)	18	0	349.7	69,940
TSM (Non-opt. reinforced)	28	0	602.4	120,480

the research space to 42 Booleans ($dim(b)=42$), instead of 78, which encodes the topology of the reinforcements for the structure. The dimension of the design space is reduced to $2^{42} \approx 4.4\times10^{12}$ different tentative solutions instead initial dimension of $2^{78} \approx 3.02\times10^{23}$.

The GA routine was run with an initial population (P) of 200 tentative random solutions. The algorithm proceeded by generating 200 new children per generation through parent selection, crossover, and mutation operators. A tournament size $k=3$ was used for the parent selection. The mutation probability (p_m) was set as 5%. The penalty coefficient (p) to be used in Eq. (11), was calibrated with a few trial analyses, which gave better results by setting $p=5$. Stopping criteria have been set to a maximum of 25 generations (G_{max}) and a stall of 10 generations (S_{max}), representing the maximum number of generations in which the algorithm does not improve the optimal solution. GA parameters set-up is summarized in Table 6.

The convergence history of the optimization carried out with the proposed GA routine for the SSM and TSM structures is shown in Figs. 16 and 17 in terms of the objective

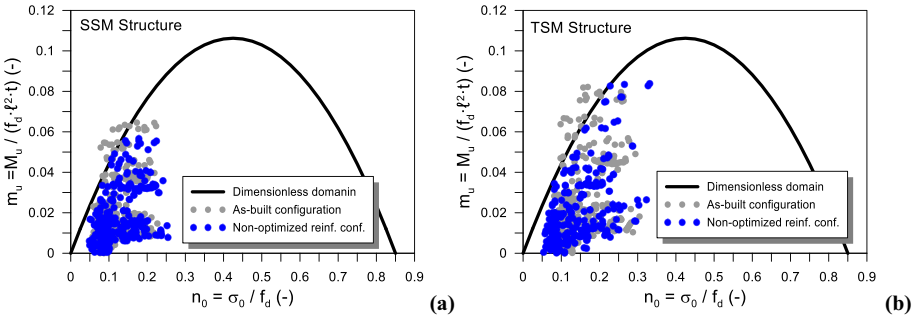

Fig. 13 Flexural safety checks for the as-built and non-optimized reinforced structures: **a** Squared stone masonry (SSM); **b** Tender stone masonry (TSM)

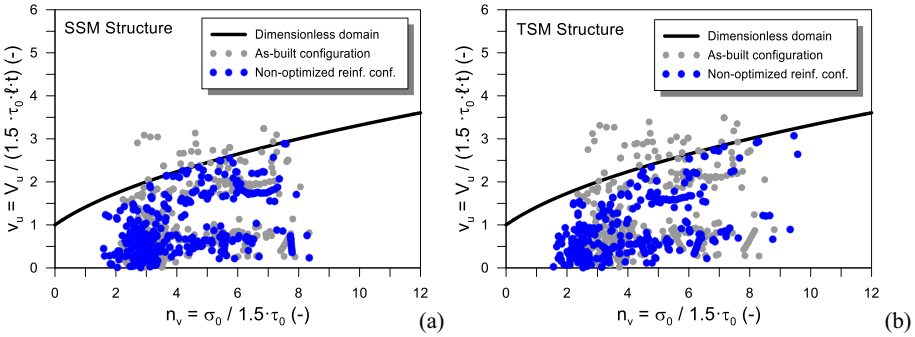

Fig. 14 Shear safety checks for the as-built and non-optimized reinforced structures: **a** Squared stone masonry (SSM); **b** Tender stone masonry (TSM)

function values (surface of walls subject to retrofit) and the number of retrofitted clusters per individual.

As can be observed from Fig. 16a and b, the optimal solutions were found in the 23rd and 18th generations for the SSM and TSM structure respectively. In both cases, the exploration phase, in which the algorithm investigates roughly the research space seeking the general characteristics of the fittest individuals, was rather steep. It is noteworthy observing that the tender stone masonry case, despite starting from higher fitness values, converged five generations earlier. Further considerations can be made by observing the exploitation

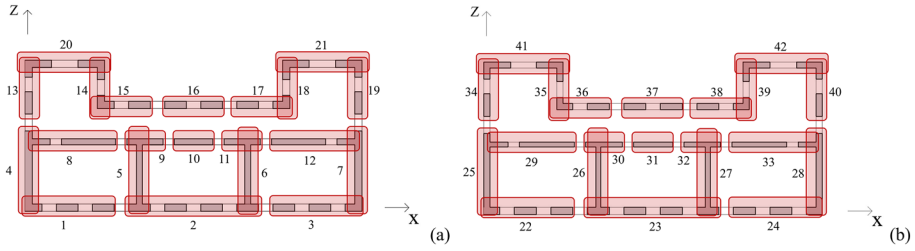

Fig. 15 Subdivision of the walls within the clusters: **a** ground storey; **b** first story

Table 6 GA setup parameters

Dimension of the design vector	Population size	Number of offspring	Tournament size	Mutation probability	Max generations	Max stall
$dim(b)$	P	O	K	p_m	G_{max}	S_{max}
42	200	200	3	5%	30	10

phase, where it can be noted that the algorithm maintains a certain diversity over the generations. This allows the algorithms to have the possibility to improve the optimal solution without getting stuck into local minima. The computational time was approximately 1.6 h to complete the optimization routine using a standard computer, meaning approximately 1 second to analyze and assess each candidate solution.

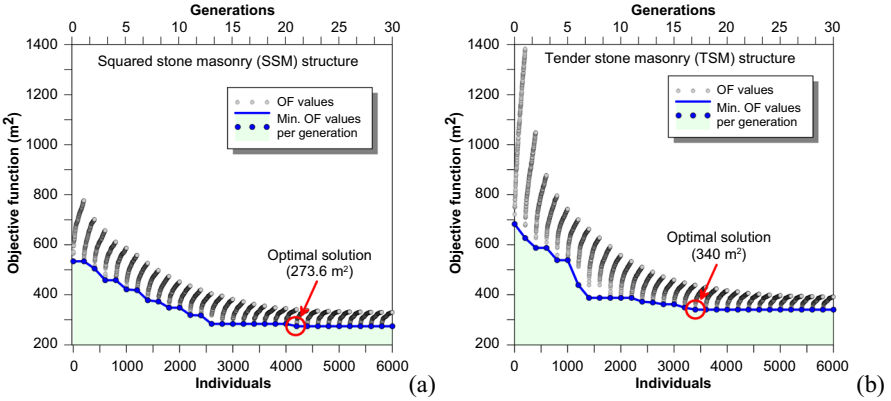

Fig. 16 GA optimization convergence history: **a** Squared stone masonry (SSM); **b** Tender stone masonry (TSM)

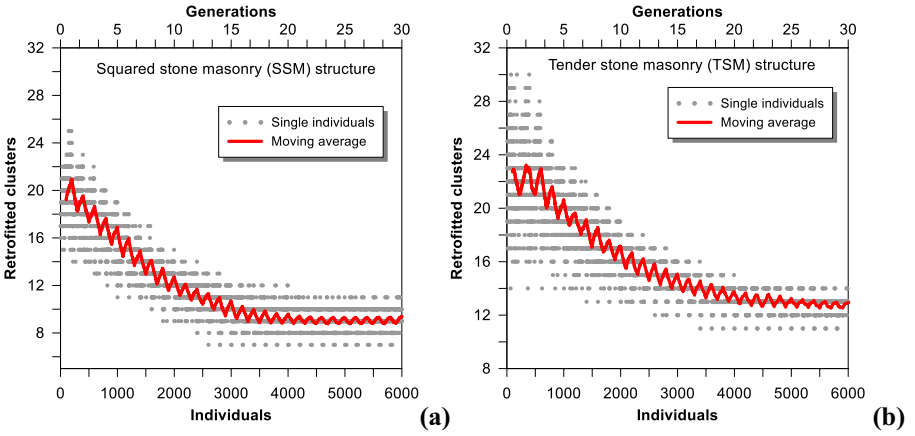

Fig. 17 Number of retrofitted clusters during the optimization history: **a** Squared stone masonry (SSM); **b** Tender stone masonry (TSM)

The optimal retrofit configurations found for the two case studies are depicted in Fig. 18. For the squared stone masonry structure case the total optimized surface of reinforced plasters was 273.6 m^2. Reinforced clusters were 8, out of 42, with a total of 12 walls out of 78. As regards the tender stone masonry structure case, characterized by poorer strengths the total optimized surface of reinforced plasters was 340 m^2 for 11 clusters, out of 42 and 19 walls out of 78. From Fig. 18 it can be also observed that, for both cases, the optimal retrofitting solutions found through the GA are also satisfactory from an engineering point of view. In fact, the proposed retrofitting configurations do not provide scattered reinforcement of the walls, but these tend to be concentrated in some specific areas. Also, the two-reinforcement layouts approximately reflect the symmetry of the structures along Z direction, confirming that a correct application of the framework can lead to reasonable engineering solutions. The slightly asymmetric layout of the reinforcement is justified by the fact that the optimization algorithm addresses the minimum cost configuration while changing the strength, and particularly the stiffness of some walls. This introduces some plan irregularity and so the optimal solution from the economic point of view may not result in a symmetrical reinforcement layout.

A further consideration about the optimization algorithm's effectiveness can be done by observing the trend of reduction of the average wall surface of reinforced walls. Figure 19 shows the ratio between the moving average of the overall surface of reinforced walls over the generations and the maximum average surface of reinforced walls. It can be observed that for the SSM structure the average area of reinforcement was reduced by 53% with respect to the average of the initial population, while for the TSM structure, the same reduction was 68%. This result denoted the major effectiveness of the algorithm in optimizing the reinforcement of the TSM structure despite the average reinforcement demand for this structure being higher. Safety checks for the structures with the optimized reinforcements are represented with the dimensionless diagrams in Figs. 20, 21. The latter are overlapped with those of the non-optimized reinforced structures and the as-built structures.

By comparing the optimal retrofitting solutions of SSM and TSM structures with the non-optimized retrofitted ones (consisting of the reinforcement of all the walls that were not passing safety checks), a significant reduction of the surfaces subject to reinforcement was found. In detail, the area of reinforced plaster for the SSM structure passed from 349.7 m^2 to 273.6 m^2 for the non-optimized and optimized retrofitted cases respectively, with a reduction of − 21.8%. As regards the TSM structures, a major gain was obtained by the application of the proposed

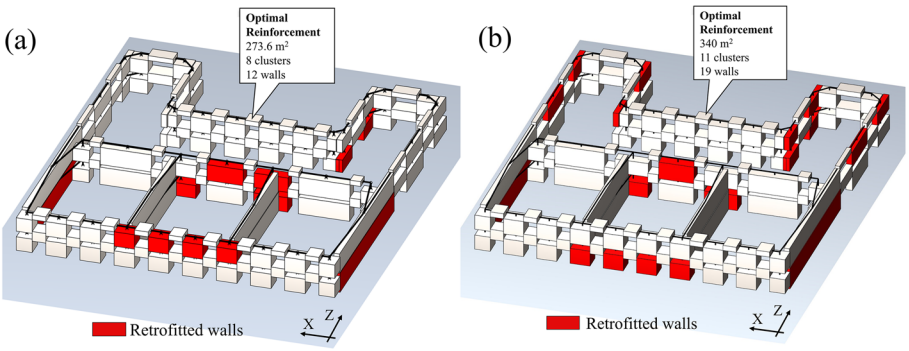

Fig. 18 Optimal reinforcement layouts for the case studies: **a** Squared stone masonry (SSM); **b** Tender stone masonry (TSM)

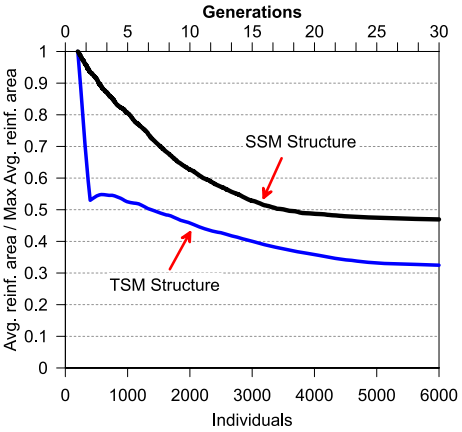

Fig. 19 Trend of the ratio between the moving average of the overall surface of reinforced walls and maximum average surface of reinforced walls during the retrofitting optimization of the two case studies

optimization framework. In fact, the structure passed from 602.4 m^2 of reinforced plasters needed for the non-optimized case to 340 m^2 for the optimal configuration. In this case, the reduction was −43.6%. Still assuming a unitary retrofitting cost of 200 €/m^2 the optimal solution found for the SSM structure had a total cost of 54,720 € instead of 69,940 € needed for the reinforcement in the non-optimized case. Considering the TSM structure, the retrofitting cost of the optimal solution was 68,000 € instead of 120,480 € resulting in the non-optimized case. It is noteworthy observing that, in both cases, the proposed framework was able to pinpoint more effective retrofitting solutions, in terms of costs and the surface of reinforced walls (Fig. 22 and Table 7). This reduction was much more significant for the tender stone masonry case study structure, which was much more vulnerable to earthquake loads because of the poorer strengths. A general consideration can be drawn from this result. What has been observed is that the application of such a kind of computational intelligence tool is much more helpful in more complex cases, namely where the difference between a non-optimized configuration retrofitting configuration and an optimized one can be relevant. Namely, if safety checks are not passed for a limited percentage number of walls, the adoption of an optimization algorithm could not bring an evident gain. On the contrary, the adoption of genetic algorithms optimization frameworks, like the one illustrated in this paper, could make the difference in terms of intervention cost and invasiveness reduction, and therefore on the quality of the retrofitting design.

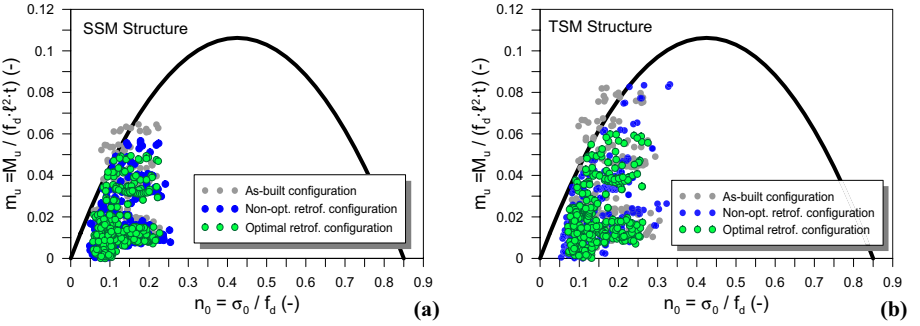

Fig. 20 Flexural safety checks comparisons of the as-built structure and non-optimized and optimized reinforced structures: **a** Squared stone masonry (SSM); **b** Tender stone masonry (TSM)

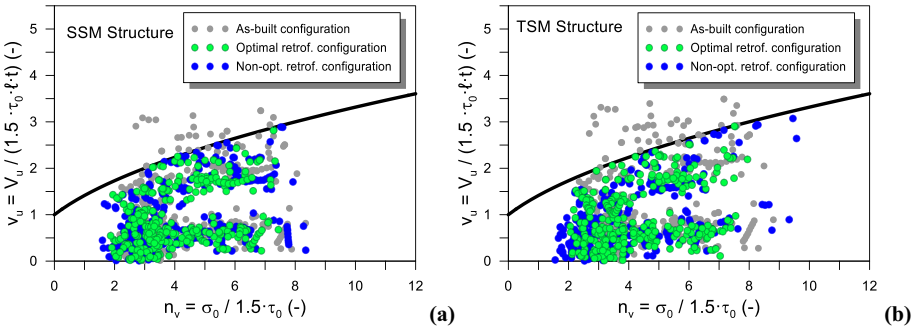

Fig. 21 Shear safety checks comparisons of the as-built structure and non-optimized and optimized reinforced structures: **a** Squared stone masonry (SSM); **b** Tender stone masonry (TSM)

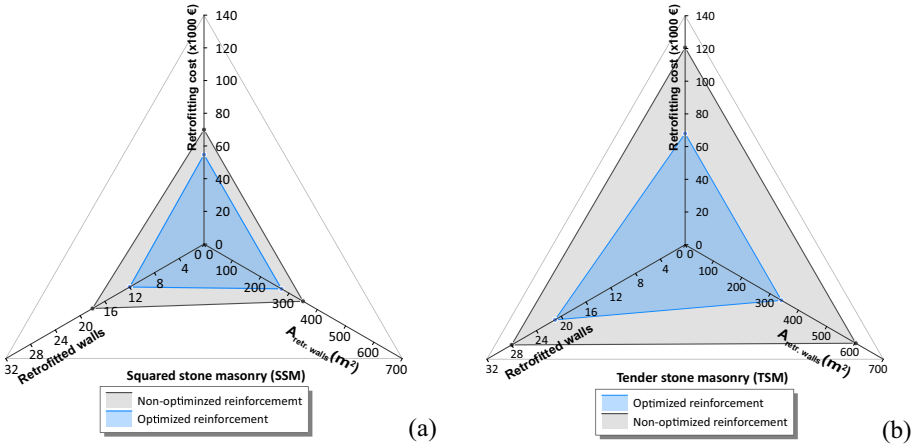

Fig. 22 Shear safety checks for the as-built and non-optimized reinforced structures: **a** Squared stone masonry (SSM); **b** Tender stone masonry (TSM)

Table 7 Results of the optimization procedure compared with the not-optimized configuration

Case study	Retrofit design	Total surface of reinforced plasters (m^2)	Retrofit cost (m^2)	Cost percentage reduction (%)
SSM	Non-opt. retrofit	349.7	349.7	−21.8
	Optimal retrofit	273.6	273.6	
TSM	Non-opt. retrofit	602.4	349.7	−43.6
	Optimal retrofit	340.0	273.6	

6 Conclusions

The paper has shown a novel computational intelligence-based optimization framework for the topology optimization of reinforced plaster reinforcement interventions in existing masonry structures subjected to seismic loads. The optimization routine combined a genetic algorithm developed in MATLAB®, with a FE model developed in OpenSees. The

optimization algorithm was tested with a case-study structure, supposing the two sub-cases of average quality masonry (squared stone unit masonry) and poor quality masonry (coursed tender stone masonry). Results were compared with those from a non-optimized design of reinforcements (providing the retrofit of all the walls which were not satisfying safety checks). Based on the obtained results the following major conclusions can be drawn:

- The proposed optimization framework can effectively provide topology optimization of reinforcements in existing masonry structures associated with the minimization of seismic retrofitting costs.
- The algorithm can properly tackle the optimization problem with the proposed penalty approach despite handling the results of multiple seismic structural analyses and safety checks for each tentative solution.
- Both the SSM and TSM case study tests resulted in a significant reduction of the reinforced walls needed to accomplish safety checks. In particular, a major gain was obtained for the structure with poorer masonry, where a reduction of -43.6% of reinforcements was obtained. This demonstrates the robustness of the algorithm with respect to a potentially different demand for reinforcements as a function of the intrinsic vulnerability of a structure.
- Linear elastic analysis allowed reducing the computational effort of the optimization procedure. The designer could possibly test the outcomes with a more refined structural analysis method (e.g., non-linear static analysis).
- The computational burden was affordable for the investigated case study, being approximately 1.6 h with a standard computer. However, this largely depends on the dimension of the design vector and on the possible use of parallel computing.
- The outcomes of this kind of optimization algorithm should be intended as a preliminary design tool to assist practitioners in individuating cost-effective configurations of the retrofit interventions even for complex structures. Further improvements and generalizations of the proposed approach can include more design variables and local out-of-plane safety checks of masonry piers.
- A comparative study between linear and nonlinear static-based optimization of seismic reinforcements would be desirable to strike a balance between computational effort and cost savings.

Acknowledgements This manuscript reflects only the authors' views and opinions and the Ministry cannot be considered responsible for them.

Funding Open access funding provided by Politecnico di Torino within the CRUI-CARE Agreement. This study was carried out within the «AI-ENVISERS» project—funded by European Union—Next Generation EU within the PRIN 2022 PNRR program (D.D.1409 del 14/09/2022 Ministero dell'Università e della Ricerca).

Data availability Data are available upon request.

Code availability Not applicable.

Declarations

Conflicts of interest The author declares not having conflict of interest.

References

Babaei M, Mollayi M (2016) Multi-objective optimization of reinforced concrete frames using NSGA-II algorithm. Eng Struct Technol 8(4):157–164

Braga F, Dolce M (1982) Un metodo per l'analisi di edifici multipiano in muratura antisismici. In: Proceedings of the 6th I.B.Ma.C., Rome (in Italian)

Bruggi M, Gabriele M (2015) Optimal FRP reinforcement of masonry walls out-of-plane loaded: a combined homogenization–topology optimization approach complying with masonry strength domain. Comput Struct 153:49–74

Bruggi M, Gabriele M, Alberto T (2013) Design of the optimal fiber-reinforcement for masonry structures via topology optimization. Int J Solids Struct 50:2087–2106

Bruggi M, Gabriele M, Alberto T (2014) Simple topology optimization strategy for the FRP reinforcement of masonry walls in two-way bending. Comput Struct 138:86–101

Camata G, Marano C, Sepe V, Spacone E, Siano R, Petracca M, Roca P, Pela L (2022) Validation of nonlinear equivalent-frame models for irregular masonry walls. Eng Struct 253:13755

Cattari S, D'Altri AM, Camilletti D, Lagomarsino S (2022) Equivalent frame idealization of walls with irregular openings in masonry buildings. Eng Struct 256:114055

Chaves LP, Cunha J (2014) Design of carbon fiber reinforcement of concrete slabs using topology optimization. Con Build Mater 73:688–698

European Committee for Standardization. Eurocode 8 (2004a) Design of structures for earthquake resistance—Part 1: general rules, seismic actions, and rules for buildings

European Committee for Standardization. Eurocode 8 (2004b) Design of structures for earthquake resistance—Part 3: assessment and retrofitting of buildings

Di Trapani F, Malavisi M, Marano GC, Sberna AP, Greco R (2020) Optimal seismic retrofitting of reinforced concrete buildings by steel-jacketing using a genetic algorithm-based framework. Eng Struct 219:110864

Di Trapani F, Sberna AP, Marano GC (2021) A new genetic algorithm-based framework for optimized design of steel-jacketing retrofitting in shear-critical and ductility-critical RC frame structures. Eng Struct 243:112684

Di Trapani F, Sberna AP, Marano GC (2022) A genetic algorithm-based framework for seismic retrofitting cost and expected annual loss optimization of non-conforming reinforced concrete frame structures. Comput Struct 271:106855

Falcone R, Carrabs F, Cerulli R, Lima C, Martinelli E (2019) Seismic retrofitting of existing RC buildings: a rational selection procedure based on genetic algorithms. Structures 22:310–326

Falcone R, Lima C, Martinelli E (2020) Soft computing techniques in structural and earthquake engineering: a literature review. Eng Struct 207:110269

Gattesco N, Boem I (2015) Experimental and analytical study to evaluate the effectiveness of an in-plane reinforcement for masonry walls using GFRP meshes. Construct Build Mater 88:94–104

Gattesco N, Amadio C, Bedon C (2015) Experimental and numerical study on the shear behavior of stone masonry walls strengthened with GFRP reinforced mortar coating and steel-cord reinforced repointing. Eng Struct 90:143–157

Goldberg DE (1989) Genetic algorithms in search, optimization, and machine learning. Addion Wesley, Boston, pp 102–136

Goldberg DE, Deb KA (1991) Comparative analysis of selection schemes used in genetic algorithms. Found Genetic Algorithm 1:69–93

Govindaraj V, Ramasamy JV (2005) Optimum detailed design of reinforced concrete frames using genetic algorithms. Comput Struct 84:34–48

Govindaraj V, Ramasamy JV (2007) Optimum detailed design of reinforced concrete continuous beams using genetic algorithms. Eng Optim 39(4):471–494

Holland JH (1992) Adaptation in natural and artificial systems: an introductory analysis with applications to biology, control, and artificial intelligence. MIT Press, London
Kanyilmaz A, Navarro Tichell PR, Loiacono D (2022) A genetic algorithm tool for conceptual structural design with cost and embodied carbon optimization. Eng Appl Artif Intell 112:104711
Kora P, Yadlapalli P (2017) Crossover operators in genetic algorithms: a review. Int J Computer Appl 10:34–36
Lagaros ND, Papadrakakis M, Kokossalakis G (2002) Structural optimization using evolutionary algorithms. Comput Struct 80:571–589
Mahdavi G, Nasrollahzadeh K, Hariri-Ardebili MA (2019) Optimal FRP jacket placement in RC frame structures towards a resilient seismic design. Sustainability 11:6985
McKenna F, Fenves GL, Scott MH (2000) Open system for earthquake engineering simulation. University of California, Berkley
Minafò G, Camata G (2022) An open-source GA framework for optimizing the seismic upgrading design of RC frames through BRBs. Eng Struct 251:113508
Mitropoulou CC, Lagaros ND, Papadrakakis M (2011) Life-cycle cost assessment of optimally designed reinforced concrete buildings under seismic actions. Reliab Eng Syst Saf 96:1311–1331
Italian Ministry for Infrastructures and Transportations—Ministerial Decree NTC (2018)"Aggiornamento delle Norme tecniche per le costruzioni" (in Italian)
Papavasileiou GS, Charmpis DC (2016) Seismic design optimization of multi–storey steel–concrete composite buildings. Comp Struct 170:49–61
Papavasileiou GS, Charmpis DC, Lagaros ND (2020) Optimized seismic retrofit of steel-concrete composite buildings. Eng Struct 213:110573
Pham TD, Hong WK (2022) Genetic algorithm using probabilistic-based natural selections and dynamic mutation ranges in optimizing precast beams. Comput Struct 258:106681
Priestley MJN, Seible F (1995) Design of seismic retrofit measures for concrete and masonry structures. Constr Build Mater 9:365–377
Quaranta G, Lacarbonara W, Masri SF (2020) A review on computational intelligence for identification of nonlinear dynamical systems. Nonlinear Dyn 99:1709–1761
Seo H, Kim J, Kwon M (2018) Optimal seismic retrofitted RC column distribution for an existing school building. Eng Struct 168:399–404
Squillero G, Tonda A (2016) Divergence of character and premature convergence: a survey of methodologies for promoting diversity in evolutionary optimization. Inf Sci 329:782–799
Turnšek V, Čačovič F (1971) Some experimental results on the strength of brick masonry walls. In: Proceedings of the 2nd international brick masonry conference. Stoke-on-Trent, British Ceramic Research Association, pp 149–156